

The plasma source of the Large Plasma Device at University of California, Los Angeles

D. Leneman,^{a)} W. Gekelman, and J. Maggs

Department of Physics, University of California, Los Angeles, Los Angeles, California 90095

(Received 3 October 2005; accepted 20 November 2005; published online 25 January 2006)

The Large Plasma Device at the University of California, Los Angeles has recently been upgraded. The plasma is now 18 m long (the device is 22 m long) and is designed to produce a 0.36 T axial magnetic field. Its plasma source has also been upgraded, incorporating a 1 m square heater, a 72 cm diameter cathode and anode, and associated heat shields and reflectors. The barium oxide coated cathode is heated to 750 °C and can produce plasmas of diameters up to 0.9 m diameter (depending on the magnetic field configuration), and densities up to $7 \times 10^{12} \text{ cm}^{-3}$ with a spatial uniformity of $\pm 10\%$. © 2006 American Institute of Physics. [DOI: [10.1063/1.2150829](https://doi.org/10.1063/1.2150829)]

I. INTRODUCTION

Barium oxide-coated cathodes have been used for decades in vacuum tubes and plasma research. When they are used to inject accelerated electrons into neutral gas, dense quiescent plasmas can be produced. As such, they are attractive as sources for experimental plasmas. At the Large Plasma Device (LAPD) at the University of California, Los Angeles (UCLA), there is much interest in performing plasma experiments which are relatively unaffected by the plasma boundary. Therefore, it is desirable to have the plasma ion gyroradius small compared to the diameter of the plasma. For reasonably accessible magnetic fields of 0.1 T, and for typical ion temperatures in the LAPD (1 eV), the argon-ion gyroradius is about 0.6 cm. This means that the plasma must be larger than 30 cm in diameter. Barium oxide-coated cathodes of this size are very difficult to implement because they must be heated to between 700 and 800 °C. Issues, such as differential expansion of component parts and heat loss, become problematic. Nevertheless, large sources have already been designed and implemented.¹ Sources of this size require large electrical currents for heating and can produce large emission currents; therefore, embedding them in fields stronger than 0.1 T introduces additional problems due to the $\mathbf{j} \times \mathbf{B}$ force. This is why a new design was required at the LAPD. Uniform plasma production depends on uniform cathode temperature and coating. These are also increasingly difficult to achieve as the overall size increases.

The basic layout of the most important elements of the source is depicted in Fig. 1. An oxide-coated cathode, in conjunction with a grid anode, is used to produce a large cross section electron beam. The cathode, which is capable of emitting electrons only when it is hot, must be planar. The cathode should be at least as broad as the electron beam required, and it should be thin to minimize edge heat losses and weight. As will be discussed later, very good reflectors of radiant heat are difficult to make, so in order to minimize edge heat losses, the heater must be placed near the cathode

(about 6 cm in this design), and therefore must also be planar. For uniformity of heating, the heater must be larger in diameter than the cathode. An important detail is that the efficiency of the heater can be significantly increased if the back side, i.e., the side opposite the cathode, has a heat reflector to reduce the heat loss there. The heater and reflector assemblies are mounted to a support frame (not shown in Fig. 1), which is bolted to the vacuum chamber walls.

This article describes the LAPD plasma source design and the techniques used to prepare the oxide coating. It is organized as follows: The heater, cathode, and anode assemblies are described. The heat shield, which envelops much of the heater, is subsequently discussed. Specific details of the assemblies are highlighted as solutions to problems, such as differential expansion, $\mathbf{j} \times \mathbf{B}$ forces, heat loss, heating uniformity, and ease of building and maintenance. Next, the cathode coating preparation, spraying technique, and in-vacuum conditioning are described. Finally, vacuum chamber leaks and plans for improvements of the source are discussed.

II. HEATER

The heater measures 97 by 105 cm when cold and is composed of ceramic covered metal filaments, strung in parallel between two copper buss bars. The Stefan-Boltzmann law (blackbody radiant power per unit area scales as T^4 , where T is the absolute temperature of the radiator) dictates that it is most effective to radiate heat from a thin metal filament at high temperature (about 1500 °C), rather than a thicker metal filament at lower temperature (such as nicrome which melts at 1500 °C). Of all alloys with melting points higher than 2500 °C, tungsten alloyed with 3% rhenium is the metal of choice. At room temperature, it is malleable enough to bend and cut easily (unlike molybdenum) and maintains its shape at very high temperatures (unlike tantalum). Filament deformation is a problem given the expected $\mathbf{j} \times \mathbf{B}$ forces. Because the heater must be large, and the filaments must be close together, the only reliable way to avoid electrical short circuits is to envelop them in high-temperature ceramic tubes. The ceramic of choice is alumina

^{a)}Electronic mail: leneman@physics.ucla.edu

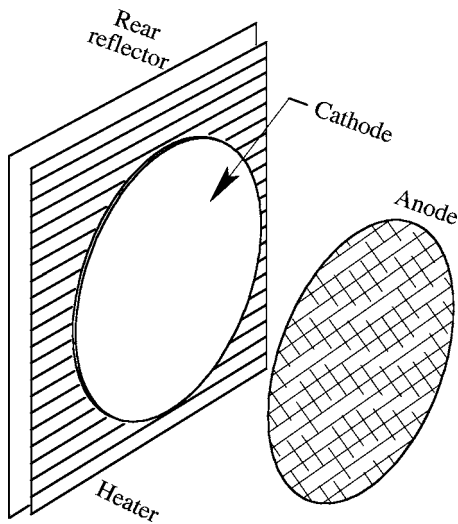


FIG. 1. The basic layout of the source's most important elements is shown: The heater, cathode, anode, and rear reflector. The cathode diameter is 72 cm and the anode-cathode distance is about 50 cm.

with 99% Al_2O_3 because of its temperature capability (1500 °C sag temperature), tensile strength, and thermal conductivity. Since heating uniformity is important, the ceramic tubes cannot be spaced too far apart. Because the rear reflector is not very efficient, radiant energy reflected back through gaps between ceramics is small compared to direct radiation. Experience shows that a 1 cm center-to-center spacing is not too coarse and a 0.5 cm spacing is not so fine as to make the heater too difficult to build. A 0.6 cm spacing was chosen, given the availability of 0.48 cm outer diameter (o.d.) ceramic and, as will be discussed later, the need for a 0.12 gap between them.

After the ceramic spacing is set, the diameter of the tungsten wires can be chosen. It is necessary to construct the insulated filaments by threading the wires through several segments of ceramic tubing. This grouping of several filament wires, which are threaded through several lengths of ceramic tube, is the building block of the heater. From this point on, it will be referred to as a heating element. Since the wires of the heating element are bent so the tubes can lie side by side, the bend radius must be one-half of the ceramic spacing mentioned above. Experience shows that wire diameters larger than 0.075 cm are problematic for these bends. The radius can be reduced if the wire is heated with a torch during bending but this increases the difficulty and time of assembly. There is also a lower bound in the selection of wire diameter because there is a minimum conductor surface area per unit length required. If one arbitrarily reduces the wire diameter, the required number of wires goes up which again complicates the design and construction. Therefore, the maximum wire diameter (0.075 cm) is used. There is another more subtle reason to keep the diameter at the maximum. Many laboratory vacuum systems, particularly large ones, such LAPD's, have a significant partial pressure (about 3×10^{-8} Torr) of residual water vapor. When tungsten reaches elevated temperatures, the H_2O acts as a catalyst in transporting the hot metal to the colder ceramic. This transport rate can be hundreds of times greater than the sublimation

rate. Since for a fixed current, the power radiated per unit length of wire scales as $1/d^2$ (where d is the diameter of the wire), and given that d is constantly decreasing, the time rate of change of the radiated power due to degradation of the filament goes as $1/d^3$. Therefore, it is advantageous to use as large a wire diameter as possible to maintain heating uniformity on a time scale of months and extend the rebuild time to a couple of years.

To settle on the number of wires per heating element, the required radiant heat flux must first be estimated. This is at most twice the total radiated flux of the cathode. The factor of 2 arises because the elements radiate toward the cathode and backward to the rear reflector (the present rear reflector is about as reflective as the cathode). The cathode also radiates in two directions, the sum, is 15 W cm^2 at 800 °C. Here, it is assumed that the emissivity equals 1 on both the front and back to design for the worst case. This means the wires must radiate 18 W cm along their length (since the ceramic spacing does not increase appreciably at operating temperature). If the tungsten is limited to operate at the sag temperature of the ceramic tube (1500 °C), then there must be enough wires to provide at least 0.80 cm^2 of radiative area per cm of conductor length to achieve the required radiated power. This calculation uses the Stefan-Boltzman law and a value of 0.4 for the emissivity of the tungsten.² Four 0.075 cm diameter wires about have 15% more radiative area per unit length than required. The ceramic tube inner diameter is 0.24 cm to accommodate these wires. In practice, this configuration—along with a filament temperature of about 1500 °C—heats the cathode to about 750 °C. If the filaments exceed 1500 °C, the ceramics exhibit chemical degradation possibly due to reactions with the tungsten alloy and the residual gases in the vacuum chamber.

How the heating elements should be configured must be determined next. An elegant way to avoid any net $\mathbf{j} \times \mathbf{B}$ force on the heater is to build heating elements using an even number of ceramic tubes positioned side by side. As such, the supply and return current buss bars must be situated close to one another on the same side of the heater. Which makes the system prone to short circuits. In any case, such a design must still accommodate the $\mathbf{j} \times \mathbf{B}$ force on each ceramic section of the heating elements. In a configuration where the tungsten wire is threaded through an odd number of ceramic tubes (see Fig. 2), the buss bars can be positioned one ceramic length apart and short circuits are avoided. The present heater incorporates elements, which are constructed by threading the tungsten wires through three horizontal ceramic tubes. As such, the net $\mathbf{j} \times \mathbf{B}$ force is reduced by a factor of 3 compared to three one-pass heater elements (same current in either case). Now it can be appreciated why bending of the conductor wires is considered at all. This construction technique is useful for two additional purposes: (1) conductive heat loss from the tungsten wires to the water-cooled buss bars is reduced, and (2) buss bar cross sections and/or resistive losses are reduced because the total current required is reduced.

To better understand the second point, consider that under normal operating conditions, 34 A of current runs in each filament. Given the three-pass configuration of the heat-

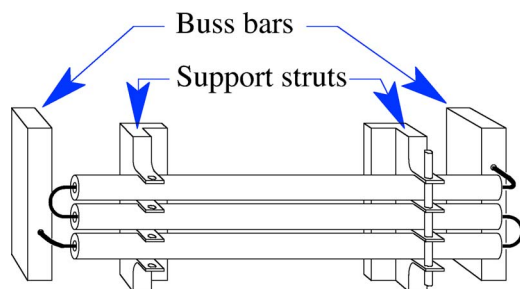


FIG. 2. Ceramic tubes, supported in molybdenum struts, are threaded with tungsten wires, which connect to copper buss bars. The grouping of three ceramic tubes with their tungsten wires within is called a heating element. Each ceramic is supported in U-shaped slots, which facilitate assembly. The closest they can be for reasonable machinability of the tabs is 0.6 cm. The strut on the right is shown with the tungsten retainer rod installed.

ing elements and the space available, there are 53 heater elements making the total required current 1.8 kA. At operating temperature, the required voltage is 28.5 V. If, for example, the heating elements were constructed using only one ceramic tube (the filaments would go directly across from one buss bar to the other), then the total operating heater current would be 5.4 kA. The buss bars for the three-pass configuration are made of a 0.6 by 2.5 cm copper bar strengthened with two aluminum ribs. As a result, the voltage drop along each buss bar is only 0.06 V.

Given the complex structure of the heater, its large current and ceramic temperature and the strong ambient magnetic field, mechanical support of the heating elements is a challenging design issue. The choice was made not to orient the ceramic tubes vertically because any successful support structure would have to accommodate the conductors where they exit the tubes. In order to avoid electrical shorts, such a support would have to be made of high strength high-temperature ceramic. This is very expensive to machine, difficult to implement with high thermal gradients, and possibly too delicate to handle during the assembly phase. Instead, the tubes are oriented horizontally and supported in “U”-shaped features machined in six vertical struts made of molybdenum. In order to highlight the most important aspects of the design, Fig. 2 shows a shortened heating element supported in two struts. The heating elements can only move within a small range in the horizontal direction because they are restrained by bends in the wires, including bends where the wires emerge from the elements and head to the fixed buss bars. The ceramics are restrained in the U’s by a tungsten rod which is threaded into holes in the tabs separating each ceramic. This open design is chosen for ease and speed of rebuild. Also, with this design, if one element fails, it can be extracted and a replacement inserted. With the help of a specially designed bending fixture used to manufacture the heating elements, a heater rebuild takes only 20 man hours. Without this open design, the elements must be manufactured in place and the ceramic tubes need to be installed before threading the wires. But threading the wires in fixed tubes produces extraneous bending, which is difficult to remove and renders them too unwieldy to fit in the bores.

The maximum magnetic field capability of the LAPD is 0.36 T. However, the field strength at the heater location

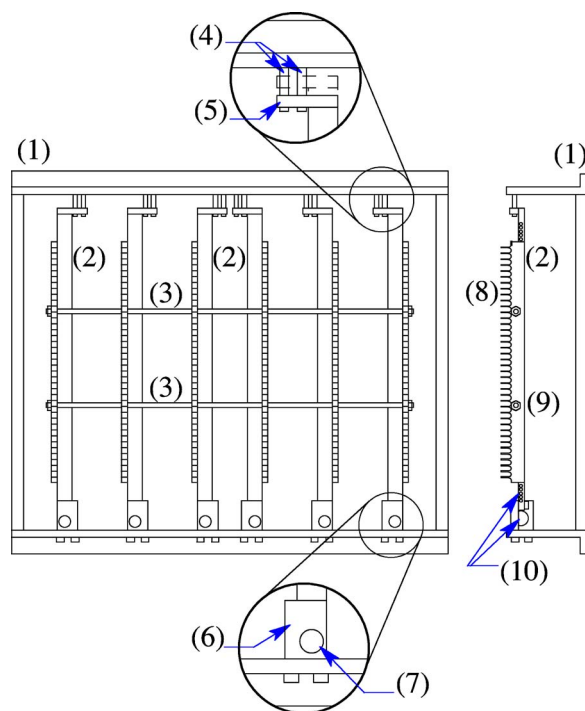


FIG. 3. The heater support structure is shown, but the components are not to relative scale. The assembly is comprised of the frame (1), and molybdenum support struts (2), which include tungsten retainer rods (shown in Fig. 2). The strut cross section is L-shaped and 0.6 cm thick. The lateral support struts are tied together with horizontal molybdenum tie rods (3), which are threaded through holes in the medial struts. The top detail shows an expansion joint. It consists of two guide rods (4), which protrude through holes in a tab (5) at the top of the struts. The joint is redrawn in dashed lines to show the position of the tab and top of the strut in when the heater is at operating temperature. Bottom detail shows a stainless-steel mounting bracket (6) with a hole (7), which reduces heat conduction from the heater to the frame. In the side view, the U-shaped openings (8), which support the ceramic tubes (not shown), are visible as well as the nuts (9), which secure the ends of the molybdenum tie rods, and more holes for heat conduction reduction (10).

(near the end of the magnetic solenoid) is 0.22 T. Given the operating current, the maximum force density is 7.5 N per meter of conductor length. Since the ceramic tubes are supported at 20 cm intervals, the relevant stress is 1.5 N over this span. The maximum net force on the entire collection of ceramics is less than 420 N. The two middle struts (see Fig. 3) must support up to 140 N each. This may not seem like a lot but one must keep in mind that the struts and ceramics attain a temperature of about 1000 °C. To date, the heater has been tested up to a local field of 0.11 T. At this field, the struts and ceramics bow minimally.

Other important design aspects of the support struts are: (1) They must not conduct significant heat away from the heater because they are in thermal contact with a cold support frame (see Fig. 3). To reduce the conductive heat loss, several design features are employed. There are several small holes drilled sideways through the struts (see side view of Figs. 3 and 4). Because the holes mechanically weaken the struts, they are placed where the struts are cool, i.e., where the struts protrude outside the heat reflectors (discussed below). Very little heat is conducted past the expansion joint (described below) at the top of the strut. The bottom of the strut is attached to the frame with a stainless-steel bracket (see Fig. 3 detail). The choice of bracket material and the

additional holes both reduce heat conduction. (2) There must be a provision for the predicted 0.6 cm expansion along their length. To accommodate this, there is an expansion joint at the top of each strut. The joint consists of two rods which extend down from the support frame and which engage a tab attached to the top of each strut (see top detail of Fig. 3). (3) As the ceramics expand, there is potential for binding since they may bow and the struts may twist. To minimizing this possibility, the U-shaped openings are relieved at the arc of the U.

This design is successful in that the ceramic tubes move freely in their supports and do not break as the heater warms. However, in trials with less robust struts, the tubes exert enough frictional force to cause the lateral struts to bow sideways (i.e., in the tubes' axial direction). To solve this problem, the lateral struts are tied together at several locations with 0.38 cm diameter molybdenum rods. To avoid other deformations of the struts, the tie rods are routed through holes in the medial struts so they run in a straight line from one lateral strut to the other (see Fig. 3).

The $\mathbf{j} \times \mathbf{B}$ force must also be considered for the heater buss bars. Since the current in the buss bars varies over the their length, and since the magnetic field is flared where they are located, the total force was numerically calculated. The results for maximum magnetic field (0.36 T in the solenoid) and maximum bus bar current (2.0 kA) are as follows: 97 N in the direction along the width of the bar; 96 N in the direction along the thickness of the bar (the weakest direction). The center of force is about 13 cm above the middle of the buss bars. The force aligned with the length of the buss bars is negligible. The force along the weak direction is large enough to warrant reinforcement of the buss bars. As mentioned above, the reinforcement takes the form of two aluminum ribs with a 0.6 by 1.3 cm cross section running the length of each buss bar.

Differential expansion is an issue that must be dealt with in several other aspects of the heater design. Under normal conditions, there is no problem with differential expansion between the tungsten wire filaments and the alumina ceramic tubes. Even though the thermal expansion rate for alumina is about 20% greater than that of tungsten, the former is normally cooler than the latter. At their estimated operating temperature of about 1000 °C, the ceramic tubes expand 0.8 cm lengthwise while the tungsten wire (at 1500 °C) in those tubes expands 0.75 cm. However, a problem arises if there is a power outage or if the heater must be powered down rapidly (because a vacuum leak is detected, for example). In this case, the tungsten thermally equilibrates with the ceramic and then the difference in expansion rate matters. For this reason, the straight sections of wire are at least 0.3 cm longer than the tubes.

Another area that requires attention is the differential expansion of the ceramic and support strut assembly versus the thermally stable water-cooled buss bars. For ease of assembly, the wires are connected directly to the buss bars, by bolting them down with machine screws. Because the ceramics expand horizontally (along their length) and are forced upward as the struts expand vertically, the end sections of wire must be able to accommodate a variable distance be-

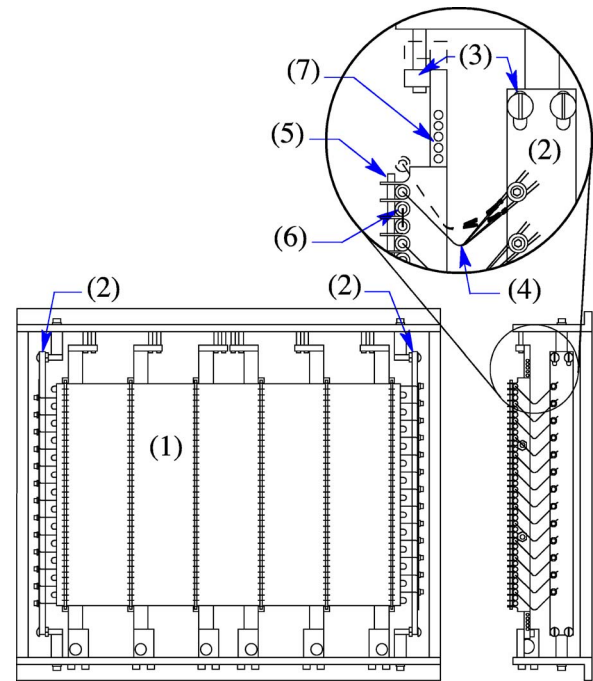


FIG. 4. The heater assembly is depicted installed in the support structure. It is comprised of a stack of heating elements (1) and two buss bars (2). The components are not to relative scale. The ends of the filaments are attached to the buss bars. The detail of the side view shows the expansion joint (3) of a lateral strut, a buss bar, (2) a 90° bend (4), at the filament end of a filament and the screws and washers used to attach the filament ends. The filaments deform as the struts undergo thermal expansion. The top most filament and ceramic tube are redrawn in dashed lines to show the displacement and the filament deformation as a result of the thermal expansion of the support struts. Similarly, the top of the strut is redrawn. Also visible in the detail is the top of a tungsten retainer rod (5), an end view of retained ceramic tubes (6), and some of the holes (7) drilled in the struts to reduce heat conduction to the frame. The reflector and heat shield assembly (not shown) are supported by the frame. The support struts and filaments protrude through holes in these barriers, which otherwise envelop the heater elements.

tween the ceramic ends and the attachment points on the buss bars. The variable distance is accommodated by introducing a 90° bend in the wire ends (see Fig. 4 detail) to provide the required flexibility. Brass washers are used as an intermediary between the tungsten wires and the buss bar to prevent the soft copper from getting embossed with the wire form. This makes a heater rebuild more reliable, since using new washers renews the contact areas.

There is also an expansion issue for the buss bars relative to the mounting frame. Even though the buss bars are water cooled, the frame is not. And since the heat shields have gaps, and conduction of heat through the struts is not zero, the frame reaches an average temperature of 60–80 °C. Even though the difference in expansion is small the overall lengths are large, and since the buss bars must be electrically insulated they have ceramic mounts, which are brittle. In addition, if there is an accidental deficit of cooling water, the heater current will automatically be interrupted, but there is still enough stored heat to cause the buss bars (among other assemblies) to expand significantly as the temperature of the entire assembly equilibrates. Therefore, the buss bars are mounted using slotted holes at the top (see Fig. 4 detail).

III. CATHODE

The substrate material commonly used for barium oxide cathodes is nickel. The combination must be heated in order to emit electrons at reasonable voltages (less than 100 V). The alloy of nickel used deserves some discussion. Many researchers have studied how impurities in the nickel can significantly affect the electron emissivity of oxide-coated nickel cathodes. Kohl³ singles out aluminum, chlorine, silicon, and sulfur as deleterious and specifies that the sulfur content must be less than 0.005%. Nergaard⁴ recommends that silicon be held below about 0.01%. Kohl³ rates several alloys of nickel. The ones with the best and most consistent emissivity have these specifications: Ni \geq 99.0%, C 0.08–0.10%, Cu 0.10%, Fe 0.10%, Mg 0.01–0.10%, Mn 0.2–0.3%, S 0.008%, Si 0.01–0.05%, and Ti 0.005–0.05%. Iron, copper, and cobalt are believed to be inert in the presence of barium oxide, and tungsten has been added in some alloys for strength. To date, nickel sheet from three separate melts have produced satisfactory cathodes at the LAPD. The material test report (provided by the vendor) for one of them states that the composition (in %) is: Ni, 99.56; C, 0.10; Cu, 0.10; Fe, 0.10; Mn, 0.14; S < 0.001, and Si, 0.04. The material was ordered with the request that the alloy meet the American Society for Testing and Materials (ASTM) Specification B162. This specification allows for more silicon and sulfur than Kohl³ and Nergaard⁴ recommend; nevertheless, the experience at the LAPD is that the test reports show tolerable levels. While this experience gives a measure of confidence that the B162 specification is sufficient for cathodes, it is recommended that the test report be examined for sulfur and silicon before purchase.

Four major engineering issues impact the cathode substrate design. These are thermal expansion, the impulsive $\mathbf{j} \times \mathbf{B}$ force due to the pulsed plasma discharge current in the presence of a magnetic field, voltage drop through electrical connections and the nickel sheet itself, and temperature uniformity. One design feature addresses the first two concerns: The sheet is springmounted in a support frame (see Fig. 5 and detail A). The spring suspension accommodates the expected 0.51 cm thermal expansion of the cathode at 750 °C and absorbs the energy produced by the impulsive $\mathbf{j} \times \mathbf{B}$ force as well. Copper braid is used for the electrical connection to the nickel. This flexible connection can survive many mechanical cycles due to the $\mathbf{j} \times \mathbf{B}$ force.

The annular frame to which the suspension springs are attached is water cooled because it must block the radiant heat, which would otherwise impinge on the rest of the machine, the springs, and copper braid. If the springs or braid were to attain elevated temperatures, the springs would sag, and the braid would fatigue and break. These parts are further insulated from high temperatures because they do not make direct contact with the hot part of the nickel sheet. Instead, the sheet has extension tabs (see Fig. 5 and detail A), which are also shielded from radiant heat. The insulation works both ways: If the braid were attached directly to the edge of a disk, significant heat would be conducted away and cathode temperature uniformity could be compromised.

The cathode frame is supported by four water-cooled

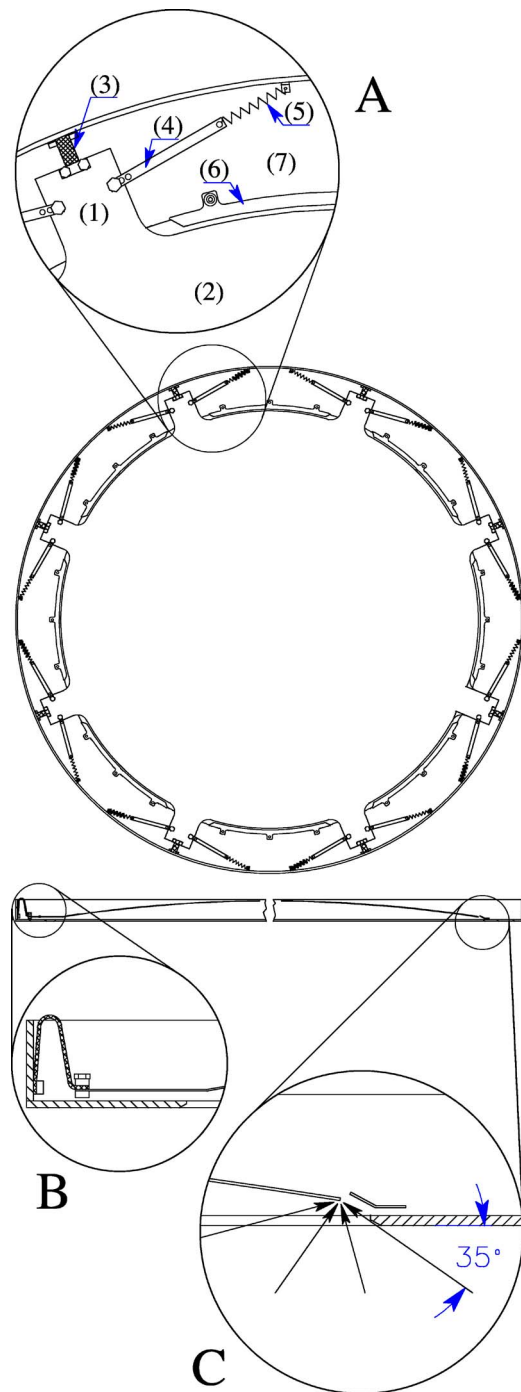


FIG. 5. The cathode assembly (side facing away from the heater) and cross sections are shown with components to relative scale. The assembly is comprised of a nickel sheet suspended by springs in an annular frame. Detail A shows an extension tab (1) of the nickel sheet (2), which thermally insulates the copper braid electrical connection (3) from the hot part of the sheet; and an extension strip (4), which further insulates a suspension spring (5). The strip has extra holes for fine adjustment of cathode position. Also visible, is part of a crescent reflector (6), which blocks heat from escaping through the gap between the nickel sheet and the cathode frame (7). The cross section shows how the cathode nickel bows when hot. The left half of the cross section is a radial slice through an extension tab. The right half is a radial slice between tabs so the details of the gap between the nickel sheet and the frame can be seen. Detail B shows how the copper braid is attached to the cathode and frame; it has extra length to reduce flexing when the nickel tab moves torsionally (in and out of the page) due to the $\mathbf{j} \times \mathbf{B}$ force. Detail C shows how the cathode edge receives all but 35° of the most oblique rays from the heater and how the crescent reflector is situated to block radiant heat.

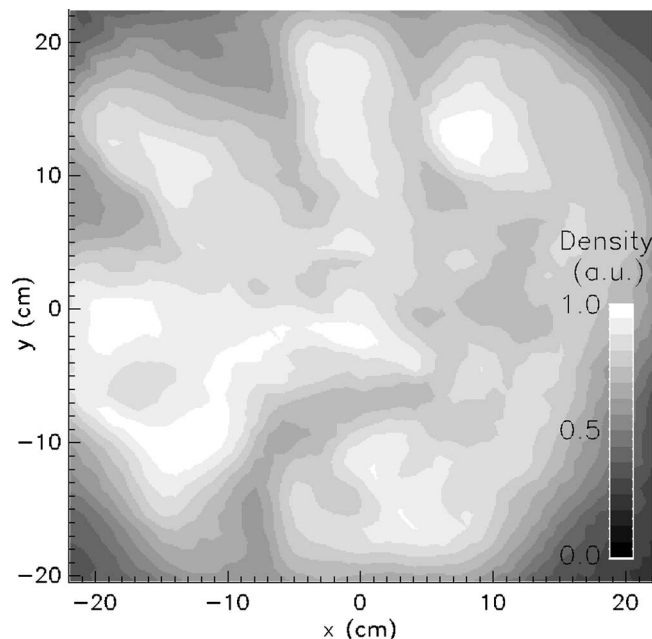


FIG. 6. This plot uses a gray scale to represent the electron density across an actual plasma column produced by the LAPD's plasma source. The plot is centered on the symmetry axis of the LAPD's magnetic field, as is the center of the cathode.

buss bars, which carry discharge current gated by a transistor switch.⁵ One of the buss bars also incorporates the supply and return passages for the cathode frame cooling water. Electron current flows from the buss bars to the frame, and then to the cathode via the copper wire braid sections. These parts must be cool to keep the voltage drop of the plasma discharge current supply at a minimum. The current is distributed into eight connections evenly spaced around the cathode (see Fig. 5 and detail B). For even distribution, it is important that the voltage drop around the frame be much less than that in the braid and extension connection. There is also a radial voltage drop in the nickel sheet itself. This is more critical than the drop in the current path to the nickel, because it bears directly on plasma production as a function of radius. The thicker the sheet, the smaller the radial voltage drop. On the other hand, the thicker the sheet, the more difficult it is to suspend. A compromise is achieved with a thickness of 0.075 cm: The expected radial voltage drop for 10 kA of discharge current is only 0.35 to 0.5 V (depending on how the emitted electron current is distributed). This is comparable to the radial voltage drop in the anode, and the combination is small enough that no central depression appears in the plasma column.

Cathode temperature uniformity is very important for uniform plasma production, because the electron emissivity of the oxide-coated cathode is an exponential function of temperature. In tests of prototype heaters irradiating nickel sheets, temperature variations of about 40 °C were observed, over about 4 cm distances. These may have been due to local variations of the heater. Similar nonuniformities may cause the observed plasma density variations on the 3 cm scale (see Fig. 6) but a Fourier analysis of the density profile shows that most of the variation is on a 7 to 8 cm scale. Since the cathode sits in a flared magnetic field, these varia-

tions are 8–10 cm when projected back to the cathode. One way to address possible 4 cm variations in the heater output is to use a thicker nickel sheet, however, smoothing only becomes significant for thicknesses greater than 0.2 cm, and the present spring suspension cannot handle the increased weight. Also, previous experience shows that thicker sheets develop a tenacious warp after heating which makes spray preparation (see below) difficult. Four cm scale variations are addressed by placing the cathode about 6 cm from the heater. Other possible causes for plasma density variations will be discussed in the improvements section below. Temperature uniformity at the edge of the cathode is addressed in the cathode frame design. Its geometry ensures that the cathode edge will receive no less than 91% of the radiative flux that the middle receives (assuming a uniform heater). This limit means that a cathode which is 800 °C at its middle, will be no less than about 775 °C at its edge. Temperature uniformity also affects cathode flatness and, in extreme cases, flatness itself can affect plasma uniformity. Calculations show that the middle of the cathode will bow in or out only 3 to 4 cm as a result of such a temperature gradient out to the edge. As mentioned, the frame shields the extension tabs, springs, and braid from radiant heat, but the tabs cannot be so close that they make contact or else severe wear will ensue due to friction and arcing. Therefore, the nickel sheet must be displaced away from the frame and, as such, if the frame opening were the same size as the sheet diameter, the sheet edge would receive only 50% of the total possible flux from the heater. In order to receive at least 91% flux, the inner diameter of the frame must be larger than the diameter of the nickel sheet, so that the frame blocks no more than 35° of the most oblique infrared rays from the outer reaches of the heater (see Fig. 5, detail C). Of course, this means that there is significant gap between the edge of the sheet and the inner edge of the frame, through which the heater energy can escape. Adding crescent-shaped reflectors at the frame's inner edge, between the cathode extension tabs, reduces this outflow. The reflectors are angled so as not to block the oblique rays discussed above (see Fig. 5, detail C). Figure 7 is a photograph of the heated nickel sheet. The uniform color of the hot part is an indication of uniform temperature. The extension tabs are cooler and therefore darker. The crescent-shaped reflectors are not installed and the bright color of the heater is visible through the gap.

IV. ANODE

The anode is a relatively simple structure owing to the small number and degree of engineering criteria it must satisfy. It is essentially an octagonal piece of molybdenum wire mesh measuring 72 cm across. It is mounted 50 cm away from the cathode (see Fig. 1 to view the anode in relation to the other source elements), and is held in a water-cooled octagonal frame. It is clamped to the frame with strong bars, thereby reducing the number of mounting bolts allowing for easier and faster mesh removal and replacement. The cathode radiates about 6 W/cm² toward the anode so its temperature would rise considerably if the anode frame were not water cooled. By keeping the extremities of the wire mesh

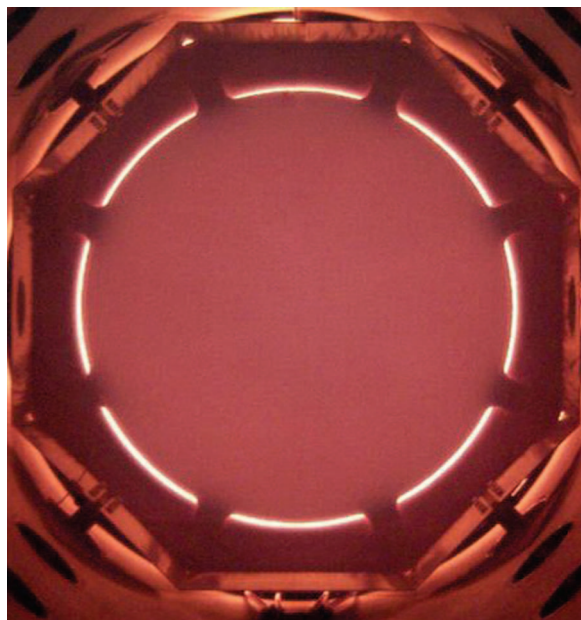


FIG. 7. (Color) The cathode assembly is photographed in situ with cathode at about 700 °C. The cooler extension tabs and extension strips are barely visible. The octagonal structure is part of the heat shield assembly, which protects the section of chamber wall between the cathode and anode. The anode and the crescent reflectors are not installed.

cool, its electrical resistance is reduced and tensile strength retained. The former is important for plasma uniformity since the radial voltage drop is reduced. The latter is important because the stress caused by the $\mathbf{j} \times \mathbf{B}$ force is concentrated at the clamps. The octagonal shape makes cutting and handling of the mesh easier.

The details of the wire mesh are important. For plasma production, experience shows that mesh transparency, must be at least 45%. But the choice of wire spacing, A , and diameter, D , is also important because it affects the radial voltage drop in the anode, and the life of the wire mesh given the stress cycles it experiences. The resistance of the mesh per unit length along its edge scales as A/D^2 and the stress per wire scales as A/D^4 (magnetic field strength and anode current being equal). But A is related to D through the transparency, which equals $(1 - D/A)^2$. Given the constraint on transparency, the resistance scales as $1/D$ and the stress as $1/D^3$. Therefore, it is favorable to use as large a wire diameter as possible (while maintaining the minimum transparency). There is however, an upper limit to D because there is an upper limit to the wire spacing: An imprint of the anode mesh on the plasma becomes noticeable if the wire spacing is larger than 0.3 cm. Several mesh geometries have been used with success. Before the upgrade of the LAPD, copper mesh made from 0.063 cm diameter wire with 0.25 and 0.30 cm spacing was used. But now, the mesh is made out of molybdenum to handle the increased temperatures due to Ohmic heating and the increased anode size. Since the plasma discharge current routinely exceeds 5 kA for 6 to 10 ms, the temperature at the middle of the anode elevates the evaporation, and sputtering rate enough to cause a copper mesh to fail after few days of use. The wire diameter

is still 0.063 cm but the spacing is 0.21 cm. As with the cathode, the expected radial voltage drop in the anode for a 10 kA discharge is between 0.35 and 0.5 V.

The cleanliness of the anode greatly affects the plasma uniformity. Therefore, whenever the cathode needs respraying, the wire mesh is sent out to a plating shop to be acid cleaned.

V. HEAT SHIELDS AND REFLECTORS

Heat shields and reflectors surround the heater. The reflectors increase heater efficiency and the shields protect the chamber walls from radiant heat. There is also a cylindrical heat shield, which protects the chamber wall surrounding the anode and cathode. The shields are made of 0.3 cm thick copper sheet and water cooled with 0.95 cm o.d. copper tubing, which is soldered to the outer surfaces at roughly 10 cm intervals. Uncooled sheet metal is used for reflectors. The shields surrounding the heater are designed to withstand an accidental fault in the cooling water supply. If the water supply fails, the heater is powered down rapidly, but the heat contained in the hot components (about 13 MJ) must be dealt with. Assuming that the stagnant water in the tubes does not turn to steam, calculations show that the temperature of the shields could rise to about 550 °C as the heater transfers its heat. This is an overestimation because, in fact, steam will form in the cooling tubes and heat will escape since the water lines are equipped with pressure relief valves. In addition, the shields also lose heat at a significant rate via radiation as they heat up (about 10 kW m² at 500 °C). Regardless, the shield supports are designed to handle the expansion due to a 550 °C temperature rise.

The efficacy of the reflectors is a very important issue. If the reflectors were perfect, the heater power required for the current operating cathode temperature (750 °C) would only be the radiated power from the cathode: Roughly 27 kW. Given the present reflectivity, the required heater output is about 55 kW. Clearly, if the reflectivity could be improved, a higher cathode temperature would be attained while operating at the same heater filament temperature. Some thought has been given to achieving higher reflectivity. Theoretically, for normally incident light at frequencies, ν , below that of ultraviolet, reflectivity from a polished metal surface is $1 - 2(\nu\rho)^{1/2}$, where ρ is the resistivity (in cgs units) of the metal. Since for most metals, ρ is roughly proportional to temperature, it is reasonable to conclude that a very good reflector could be made by water cooling a polished copper sheet. Unfortunately, this reflectivity cannot be realized in a vacuum system, which includes a heater such as this one. The heater outgases insulating material, which deposits on cooler surfaces. So much so, that within a few days time a layer accumulates, which appreciably reduces reflectivity. A chemical analysis shows that aluminum oxide is a prominent component of the deposits. Introducing two layers of sheet metal between the heater and the shields circumvents the problem. These layers are not water cooled and therefore heat up. Even though a hot reflector is less effective than a cold one (as discussed above), impurities do not deposit as readily. Adding more layers of sheet metal may improve this

scheme. Diminishing returns occur when the last layer is cold enough to collect enough deposits to become as unreflective as a cooled copper sheet. Tests have shown that two layers make the heater more efficient than one, and there are noticeable deposits on the secondary (cooler) layer. Therefore, a third layer will not be added in the future. The primary reflectors are made from molybdenum sheet. This is an improvement over the nickel sheet used in an earlier design because molybdenum has a much lower sublimation rate and significantly higher reflectivity at elevated temperatures. For example, according to the theory mentioned above, for a reflector at 600 °C, the reflectivity for molybdenum, given incident radiation with a 1 μm wavelength, is 0.84 but for nickel it is only 0.77. However, the difference is smaller given radiation at longer wavelengths: At 10 μm , the reflectivities are 0.95 and 0.93, respectively. These wavelengths are significant because 99% of the radiation from a blackbody at 1000 °C (the operating temperature of the heater ceramics) is emitted in the 1 to 25 μm range.

VI. NICKEL PREPARATION AND COATING SPRAY TECHNIQUE

In order for the nickel to emit electrons without biasing it to very high voltages or heating it to near melting temperatures, it is coated with barium oxide. A coating containing barium carbonate is sprayed on the nickel substrate and when heated in vacuum, it converts to barium oxide. Considerable effort was expended in developing a spray technique because uniformity in coating thickness and density over a large area is required.

First, the cathode coating spray material is mixed according to this formula:

- (a) 150 g Sylvania C-10 triple carbonate powder,
- (b) 225 ml binder solution, and
- (c) 225 ml amyl acetate.

The powder and binder solution are purchased from FDE Associates.⁶ The mixture is stirred for about 24 h using a magnetic stirrer. The vendor and Kohl⁴ recommend that the mixture be ball milled for 24 h, but the consistency of the spray mixture and performance of the LAPD cathode is found to be unchanged without this operation. However, the mixture can clog the spray gun if it has not been stirred long enough.

Special precautions must be taken to prepare the nickel sheet for spraying. It must be hand sanded, dry or with alcohol using aluminum oxide abrasive paper or cloth. Do not use silicon carbide abrasive because the residual particles will poison the cathode. Do not machine sand because it will drive the abrasive too deep into the metal to be removed at the final cleaning. Wipe the cathode clean with a lint-free cloth or paper and ethanol alcohol. Blow off any remaining particles with dry nitrogen. If the nickel has never been used before, it must be heated under a vacuum. This is an attempt to rid the metal of residual oils or other contamination introduced during its milling and subsequent machining. It is brought up to about 800–850 °C for about 24 h and then slowly cooled down over about a 6 h period. The nickel is

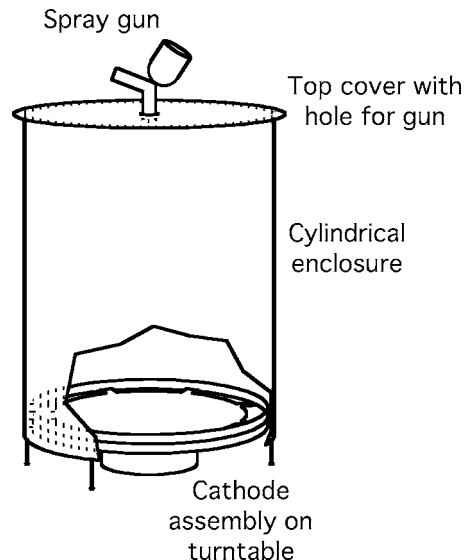


FIG. 8. The spray chamber consists of a 1.07 m diameter by 1.22 m long cylinder with its axis vertically oriented and raised above the ground by 15 cm. At the bottom is a turntable, which spins the cathode assembly and positions it 30 cm above the ground.

then sanded again as described above. Even after this process is completed, the first coating may not be viable and on occasion it detaches as it is heated.

After the cathode is prepared, the parts of the assembly where electron emission is not required are masked off. This makes for a cleaner vacuum environment and keeps the conversion time (see below) down to a minimum. In order to enhance the uniformity and repeatability of the spray, a spray chamber and high-quality spray gun are used. The spray gun must have a high-quality material delivery rate adjustment, well-engineered air passages and nozzle for thorough and drip-free atomization, and function in the spray down direction. Dry nitrogen is used as a propellant. The spray chamber is sealed on top using a clear cover with a hole in the middle to accept the spray gun nozzle (see Fig. 8). There must be enough of a seal to inhibit spray from drifting up out of the hole. The cathode assembly is placed on a turntable, and both are centered in the chamber where there is about a 6 cm radial gap between the cathode frame and the chamber wall. The chamber is raised above the ground by 15 cm and the cathode frame assembly is raised by 30 cm. These gaps allow the propellant and excess atomized mixture to flow easily out of the chamber while inhibiting contaminants from infiltrating due to ambient air currents. The turntable is necessary for spray uniformity and rotates at 18 to 20 rpm. The height of the chamber allows the spray material to spread sufficiently for a uniform deposition by the time it drifts down to the cathode. Halogen lamps are recommended as an accurate visual check is required, and they decrease the drying time. This technique affords a very uniform deposition: Thickness variations have a standard deviation of 10% over the cathode surface, and the standard deviation in density variation is 3%. Personnel spraying the cathode must wear masks with charcoal filters, as the spray material is a lung irritant and possibly poisonous.

The requisite volume of mixture is sprayed at such a rate

as to achieve a coating that, once dry, is 25 to 50 microns thick with a specific gravity of 0.8 to 1.3. To deposit this amount of coating in this setup requires 500 ml of spray mixture. But, producing the above combination of thickness and density is not straightforward. If the requisite volume is sprayed all at once, the deposition is too wet and, once dry, produces an overdense coating. On the other hand, if the spray goes on too slowly, it deposits unevenly, and conglomerates in tiny columns. To deal with this problem, a two-step spray technique is used but so far it has only been used when the ambient temperature is between 15 and 25 °C. In the first step, about 100 ml of material is applied over a 3 min period. During this phase, the delivery rate is increased every 45 s at first and later every 30 s. This is done until the coating just becomes wet. Then, the deposited material is let to dry usually about 30 to 45 min depending on ambient temperature. In the second step, the object is to get the coating uniformly wet and then stop. The delivery rate is greater than in the first step; how much depends on ambient temperature, as does duration. Usually, the remainder of the 500 ml is used up in this operation. Ideally, the small-scale structure of the coating is dissolved down in this step leaving a smooth to slightly bumpy finish. The coating is left to dry under the halogen lamps for about 1 h. Every step is affected by ambient temperature and humidity. A modified technique is now in development where the elapsed time and rate of application is set based on a practice spray. In the end, the best way to take the weather out of the equation may be to control the ambient air conditions by heating the spray chamber walls.

VII. COATING CONVERSION

Once a satisfactory coating has been sprayed, the masking is removed. If tape was used, any visible glue that remains is removed. Then, the cathode assembly is installed in its place in front of the heater, the vacuum chamber is closed and pumped down. It is very helpful if the vacuum system has a residual gas analyzer to monitor the reaction products during cathode heating. Because residual H₂O can damage hot tungsten wires, it is recommended that the chamber walls be preheated so that less H₂O is emitted once the heater reaches elevated temperatures. Heating strips strapped to the outside of the vacuum chamber are used for this purpose. In addition, the heat shield cooling water is turned off and the heater is turned on to bring the ceramic temperature up to about 100 °C. When the residual gases (which consist mostly of H₂O) have been pumped down to about 3×10^{-6} Torr, the cooling water is turned on and the heating strips are turned off. When the chamber walls cool down, the base pressure drops to about 1×10^{-6} Torr. The heater is driven up slowly so as not to let the partial pressure of H₂O rise above 3×10^{-6} Torr.

Once the cathode reaches about 350 °C, the coating begins to change chemically (at this point, the heater ceramics are at about 600 °C). Ideally, this reaction, which is commonly called conversion, consists of the transformation of carbonates of Ba, Sr, and Ca to oxides of the same, plus CO and CO₂. The cathode temperature must be throttled throughout this process, such that the residual gas pressure

(by now, consisting mostly of CO and CO₂) does not rise above 1×10^{-5} Torr. It may be beneficial to err on the side of caution and set the conversion pressure limit to 5×10^{-6} Torr. At the LAPD, this process is computer controlled wherein the total pressure is periodically sampled and the heater voltage is adjusted accordingly. Once the cathode reaches about 500 °C, conversion is mostly complete and the partial pressure of CO₂ falls relative to that of CO. Then, the cathode is superheated to 50 °C above the operating temperature for a few hours to reduce the residual gasses given off when it is brought back down. Kohl³ recommends that the cathode temperature be raised from 1000 to 1200 °C for a few minutes, for a process called activation to occur, but this would stress the LAPD heater considerably and good results are obtained without this step.

When the total pressure drops below 1×10^{-6} Torr, the chamber is backfilled with a noble gas, the magnetic field is turned on, and a pulsed voltage between the anode and cathode is applied to make plasma. The backfill gas is typically helium, neon, or argon at a pressure between 1×10^{-5} and 4×10^{-4} Torr, the magnetic field strength is at least 300 G, and the voltage pulse is 25 to 70 V. At first, the partial pressure of H₂O rises substantially, so the discharge time, voltage, and current, I_{dis} , are kept to a minimum such that a consistent discharge can still be obtained. Over about the next 6 h, as H₂O subsides, I_{dis} is increased. Once this start up phase is complete, peak plasma densities up to 7×10^{12} cm⁻³ can be achieved depending on the backfill pressure and gas. Over the next two weeks of operation, the partial pressure of H₂O drops to about 5×10^{-8} Torr. Maintaining this partial pressure or lower is recommended, otherwise the lifetime of the heater filaments (1 to 2 years) decreases. In each plasma pulse, I_{dis} first grows exponentially, then the growth slows and within 10 ms (depending on the fill pressure and gas type) I_{dis} and the plasma density peak. Normally, the discharge is terminated at this time. As such, the voltage pulses used are 5 to 80 ms long. Nergaard⁴ presents data showing that oxide coating emissivity decays during a discharge on the 30 ms time scale and a waiting period on the order of 1 s is required before full performance is restored. At the LAPD, the minimum time to acquire data is about 1 s and therefore, the plasma is pulsed at 1 Hz to maximize cathode life. In tests, discharge current densities of 6 A/cm² have been achieved but the density in normal operation is 2 to 4 A/cm².

A phenomenon, which Nergaard⁴ calls “sparking,” has been observed at the LAPD. A spark is a localized (0.1–0.5 cm diameter) bright explosive event where most of the cathode coating is blown off the cathode in the affected area. Attempts have been made to identify a threshold in either the deposition of power, energy per plasma pulse, pressure or momentum transfer due to incoming ions, but without success. To date, the rule of thumb to prevent sparks is: The discharge voltage at maximum current should not exceed 60 to 70 V for He pressure between 4×10^{-5} and 1.5×10^{-4} Torr or Ar pressure between 1×10^{-5} and 7×10^{-5} Torr. There are no such data for Ne. Even though sparking can be avoided, the constant bombardment of plasma ions cannot. This bombardment slowly sputters the

coating away and limits the coating lifetime to 3 or 4 months (assuming the normal range of plasma conditions).

VIII. LEAKS

In principle, any leak of oxygen into the vacuum chamber poisons the cathode chemistry rendering it useless over time. Poisoning is tolerated to the degree that it does not shorten the normal life of the coating. With the current vacuum pumping system, the partial pressure of oxygen is kept below 3×10^{-9} Torr. It is estimated that ten times this amount would begin to have an affect on normal coating life. Accidental air leaks can cause the level of oxygen to rise considerably. The coating can recover from an air leak, which brings the chamber pressure to 10^{-3} Torr for part of an hour. It can recover from more extreme transient leaks but a period of conditioning with a hydrogen plasma will probably be required. After such a leak is fixed, the chamber is back-filled with H_2 to about 1×10^{-4} Torr. A hydrogen plasma is pulsed for 1 to 3 h, and after which a noble gas is reintroduced to recommence normal operations. It is undesirable to use hydrogen for very long because the partial pressure of H_2O rises considerably and this can shorten the life of the heater. Also, there is some evidence that hydrogen erodes the coating at a high rate. Coatings rarely recover from leaks, which push the chamber pressure above 10^{-2} Torr.

IX. IMPROVEMENTS

Figure 6 shows a typical profile of plasma density. The full width at half maximum is typically about 52 cm. This is not a surprise since the cathode sits in a region of a flared magnetic field. The field lines intersecting the 72 cm diameter cathode coating edge compress to a 58 cm diameter where the density profile is measured. There is a noticeable plateau in the profile with a diameter of about 40 cm. Within the plateau, density varies from the average ($3 \times 10^{12} \text{ cm}^{-3}$ in this case) with a standard deviation of 10%. As mentioned before, Fourier analysis shows that the typical distance between peaks and valleys is about 7 to 8 cm; 8 to 10 cm when projected back to the cathode. Of the myriad possible explanations, three will be the focus of future modifications. In order of priority, these are variations in: (1) Cathode temperature, (2) vacuum deposition of insulating material on the anode, and (3) coating thickness and/or density. While the third issue may affect the first two, it may be the most difficult to improve. In addressing Issue (1), possible variations in heater radiation have already been considered. Addressing variations in the absorptivity of the back of the cathode nickel is the next order of business. Currently, the bare metal back becomes unevenly coated with nonconductive and

therefore absorptive deposits possibly produced by the heater. The unevenly enhanced absorption probably results in temperature variations. If the absorptivity of the cathode back could be increased with some sort of uniform absorbing coating or plating (which must be stable up to 900°C), then any subsequent in-vacuum deposition will have little effect. As such, the efficiency of heating would probably be increased as well.

As far as insulating material on the anode is concerned, inductive heating to keep the deposits from accumulating may be a solution. During conversion, there is significant deposition. Therefore, heating may only be necessary during this process since the plasma may subsequently keep the anode clean through sputtering or heating. If not, the anode may need to be periodically heated throughout the cathode's life.

In addition, a separate avenue of development is underway wherein the heater is incorporated in the cathode nickel. Commercially available high-temperature coaxial heater wire is brazed to the back side of a 3 mm thick piece of nickel. Tests with a 10 cm diameter cathode show very uniform heating. The next technical hurdle is to increase the size seven fold.

ACKNOWLEDGMENTS

The authors gratefully acknowledge Bernard Vancil at FDE Associates in Portland, Oregon for advice on coating mixture and nickel preparation and coating conversion, as well as the input and expert technical assistance of Marvin Drandel, Zoltan Lucky, and Patrick Pribyl. The LAPD upgrade was funded by a Major Research Instrument Award from the National Science Foundation (ATM-9724366). The Office of Naval Research (N00014-86-K-0611) and UCLA also provided support. Continued improvements are funded by the Department of Energy and the NSF, through the cooperative agreement for the Basic Plasma Science Facility (PHY-0075916).

¹L. Stenzel and W. F. Daley, U.S. Patent No. 4,216,405 (5 August 1980).

²*Handbook of Chemistry and Physics* (CRC Press, Boca Raton, Florida, 1987), p. E-395.

³W. Kohl, *Materials and Techniques for Electron Tubes* (Reinold, Stamford, CT, 1960), pp. 559–565.

⁴L. S. Nergaard, *RCA Rev.* **13**, 467 (1952); **13**, 469 (1952); **13**, 479 (1952).

⁵P. Pribyl and W. Gekelman, *Rev. Sci. Instrum.* **75**, 669 (2004).

⁶FDE Associates, 21070 SW Tile Flat Rd., Beaverton, OR 97007, telephone: 503-628-0703. Their formulas may be proprietary but the binder is a mixture of nitrocellulose and amyl acetate. The ASTM prescription for triple carbonate is as follows: Barium carbonate, $57.2\% \pm 2\%$; strontium carbonate, $38.8\% \pm 2\%$; calcium carbonate, $4.0\% \pm 0.5\%$; water soluble matter, 0.10% max.; iron, 0.003% max.; chloride, 0.003% max.; heavy metals, 0.003% max.; hydrochloric acid, insoluble, 0.01%.